

# Broadly tunable compact continuous-wave Cr<sup>2+</sup>:ZnS laser

Irina T. Sorokina and Evgeni Sorokin

*Institut für Photonik, TU Wien, Gusshausstrasse 27/387, A-1040 Vienna, Austria*

Sergey Mirov and Vladimir Fedorov

*Department of Physics, University of Alabama at Birmingham, 1300 University Boulevard, Birmingham, Alabama 35244-1170*

Valery Badikov and Vladimir Panyutin

*Kuban State University, 149 Stavropolskaya Street, Krasnodar 350040, Russia*

Kathleen I. Schaffers

*University of California, Lawrence Livermore National Laboratory L-482, Livermore, California 94550*

Received February 22, 2002

We report the development of a continuous-wave, room-temperature Cr<sup>2+</sup>:ZnS laser that is compact and tunable over 700 nm. The laser is pumped by a diode-pumped Er-fiber laser and generates 0.7 W of linearly polarized radiation at 2.35  $\mu\text{m}$ , at up to 40% slope efficiency. Cr<sup>2+</sup>:ZnS directly diode-pumped at 1.6  $\mu\text{m}$  yields polarized radiation that is tunable over 400 nm at up to 25 mW of output power. A comparison of Cr<sup>2+</sup>:ZnS with Cr:ZnSe (70 mW, 350 nm) in a similar setup is given. As opposed to Cr:ZnSe, the Cr:ZnS laser is intrinsically polarized. Finally, we observe sensitization of the output radiation by a few milliwatts of the visible (470–500-nm) and near-infrared (740–770-nm) radiation. © 2002 Optical Society of America  
OCIS codes: 140.3480, 140.3580, 140.3600, 140.3070, 140.5680, 160.3380.

The new class of transition-metal-doped zinc chalcogenides,<sup>1</sup> in particular, Cr:ZnSe, have attracted a lot of attention since the mid-1990s as broadly tunable continuous-wave (cw),<sup>2,3</sup> mode-locked,<sup>4,5</sup> and diode-pumped<sup>6–8</sup> lasers operating near 2.5  $\mu\text{m}$ . This interest is explained by the absence of other comparable tunable room-temperature laser sources in this spectral region. However, another member of the II–VI compound family, Cr:ZnS,<sup>1,9,10</sup> which together with Cr:ZnSe has served for the past three decades as a model object in spectroscopic investigations, has remained barely studied as a laser medium. Recently, we demonstrated the first cw room-temperature Cr<sup>2+</sup>:ZnS laser that is tunable over 280 nm near 2.3  $\mu\text{m}$ . This laser is pumped with a Co:MgF<sub>2</sub> laser and yields over 100 mW of output power.<sup>9</sup>

In this Letter we report on a cw room-temperature Cr<sup>2+</sup>:ZnS laser that is pumped by a compact Er-fiber laser and is broadly tunable over  $\sim 700$  nm. The Cr<sup>2+</sup>:ZnS laser yields up to 700 mW of output power and up to 40% slope efficiency of polarized radiation. We also report the first directly diode-pumped tunable version of this laser, which is pumped by two conventional telecommunications laser diodes at 1.6  $\mu\text{m}$ , and provide a comparison with the corresponding diode-pumped Cr:ZnSe laser.<sup>8</sup> One of the principle features that we observed in the case of Cr:ZnS and that differentiates this crystal from Cr:ZnSe is its intrinsic birefringence.

In the study reported in this Letter we used a Cr:ZnS sample grown by the physical vapor transport (PVT) method. This sample also demonstrated birefringence, similarly to Cr:ZnS crystal grown by the chemical vapor transport method (CVT).<sup>9</sup> X-ray analysis revealed hexagonal metrics in both crystals with the following lattice constants:  $a = b = 0.381$  nm,  $c = 0.935$  nm,  $\alpha = \beta = 90^\circ$ ,  $\gamma = 120^\circ$ . However, the structure of the crystals was not that of wurtzite

but was a modification of the cubic structure, with a certain degree of hexagonality (for details, see Ref. 9). Such crystals are known to demonstrate natural birefringence.<sup>11–13</sup> The lowering of the local crystalline field symmetry as a result of anisotropy may cause an increase in the oscillator strength and a corresponding lifetime decrease. Indeed, our luminescence and lifetime measurements produced a larger transition cross section and shorter room-temperature lifetime than reported earlier for cubic Cr:ZnS crystals ( $14 \times 10^{-19}$  cm<sup>2</sup> and 4.5  $\mu\text{s}$ , respectively, in Ref. 9 versus  $7.5 \times 10^{-19}$  cm<sup>2</sup> and 8  $\mu\text{s}$  in Ref. 1).

The laser cavity [Fig. 1(a)] was formed by a flat dichroic mirror, a folding mirror with an  $R = 50$  mm radius of curvature, and a plane output coupler varying from 1% to 10%. The plane-parallel crystalline plate was mounted on the room-temperature aluminum holder. The crystal of the PVT-grown Cr:ZnS was an  $\sim 2.5$ -mm-thick uncoated plate with 98% absorption at 1.6  $\mu\text{m}$ . For comparison, we used a 1-mm-thick antireflection-coated CVT-grown Cr:ZnS sample (60% absorption at 1.6  $\mu\text{m}$ ).<sup>9</sup> The diode-pumped Er-fiber laser (IPG Laser, 5-W polarized output) was focused onto the crystal by the uncoated 75-mm lens. The choice of the pump source is a crucial point for Cr:ZnS, since the absorption band of Cr<sup>2+</sup> is centered at 1.67  $\mu\text{m}$ , and only a few cw lasers are able to deliver sufficient power in this region. Alternatively, we used two InGaAsP–InP laser diodes, each providing up to 0.5 W of the output power from a 100- $\mu\text{m}$  broad stripe [Fig. 1(b)]. The diode-pumping arrangement is the same as for Cr:ZnSe,<sup>8</sup> allowing direct comparison with the present setup. Approximately 55% of the pump power was absorbed in the crystal; 34% was lost in the collimating system, and 15% was due to the reflection on the uncoated ZnS crystal surface.

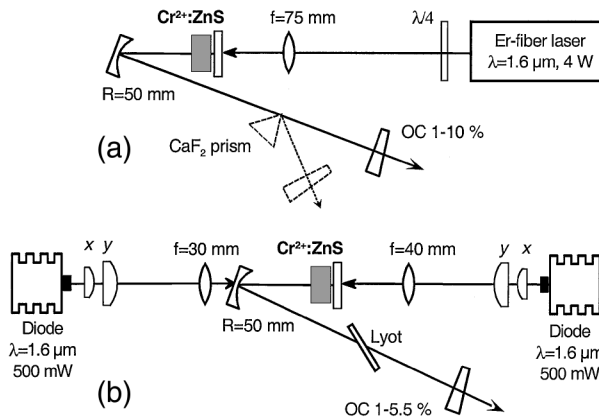


Fig. 1. Schematic diagram of the experimental setup. (a) Er-fiber laser pumped setup. (b) Diode-pumped setup. OCs, output couplers.

To explore the limits of Cr:ZnS crystals in terms of power and tunability, we first used the Er-fiber laser as a pump source. One of the characteristic features of Cr:ZnS turned out to be the fact that the laser output was always linearly polarized parallel to a certain axis, irrespective of the pump polarization. This axis corresponds to the [111] axis of the cubic structure or [001] axis of the hexagonal component. With 10% output coupler, the output power reached 700 mW at 2.65 W of absorbed pump power, with a 110-mW threshold [filled circles, Fig. 2(a)]. The excessive thermal loading prevented pumping of the laser much over 2.65 W of absorbed power. The physical mechanisms of the roll-off could be the thermal self-focusing of the pump,<sup>14</sup> thermal lensing, or lifetime thermal quenching. However, using a 1:1 chopper, we could achieve more than 1 W of output power [open circles, Fig. 2(a)] at 34% slope efficiency. This result correlates with the 40% slope efficiency found in the case of the CVT-grown sample [triangles, Fig. 2(a)], which had slightly lower losses per round trip ( $5.5 \pm 0.5\%$  versus  $7 \pm 1.5\%$ ), measured with the inverse slope efficiency analysis.<sup>15</sup> This analysis also gave a value of 63% as the limiting slope efficiency, which is close to the 68% quantum limit at 2350 nm. We thus infer that Cr:ZnS has negligible excited-state absorption, like Cr:ZnSe.<sup>7</sup> Note that in the case of the thinner CVT sample the thermal roll-off begins earlier, preventing us from pumping the laser with more than 1 W of the absorbed power. Both samples, however, sustain the same amount of absorbed power per unit length of the crystal.

Using a CaF<sub>2</sub> Brewster prism as a tuning element, we were able to demonstrate tunability over  $\sim 700$  nm from 2170 to 2840 nm [filled circles, Fig. 2(b)], using the single mirror set. Using the shorter-wavelength optics, we could extend the tuning range down to 2110 nm [open circles, Fig. 2(b)]. We believe that extension of the tuning range toward the infrared is also feasible with the use of a corresponding set of mirrors and purging of the resonator to remove water vapor [solid curve in Fig. 2(b)]. The oscillation linewidth was measured to be less than 0.4 nm ( $<20$  GHz) and was limited by the resolution of our monochromator.

Direct diode-pumped operation was realized with two pump diodes simultaneously, as shown in Fig. 1(b). The laser output characteristics in the case of the diode pumping of Cr:ZnS are given in Fig. 3(a). The threshold power of the Cr:ZnS laser was 175 mW of absorbed power (30 mW for Cr:ZnSe in Ref. 8). With 6.8% output coupler, the polarized TEM<sub>00</sub> laser output reached 25 mW at 570 mW of absorbed power and a slope efficiency of  $\sim 8\%$ , which is less than 70 mW at 460 mW of absorbed power and 17% slope efficiency in the case of the Cr:ZnSe.<sup>8</sup> The direct comparison with Cr:ZnSe is correct, as we used a similar  $\sim 2$ -mm-thick uncoated plane-parallel plate of Cr:ZnSe in the same pump and cavity configuration. The higher threshold and lower efficiency are obviously due to higher losses of our Cr:ZnS sample. We were also able to demonstrate diode-pumped operation of the CVT-grown Cr:ZnS crystal, but because of the low absorption and pump reflection on the crystal surfaces, the maximum output power was only 1.1 mW.

Using a birefringent (Lyot) filter made from crystalline quartz as a tuning element, we could demonstrate smooth tunability over 400 nm, from 2250 to 2650 nm [filled circles, Fig. 3(c)]. To our knowledge, this tuning range is the broadest ever demonstrated in the diode-pumped chalcogenides. For comparison, the tuning curve of the Cr:ZnSe sample under the same conditions is shown [open circles, Fig. 3(c)].<sup>8</sup> The structure of the tuning curves is due

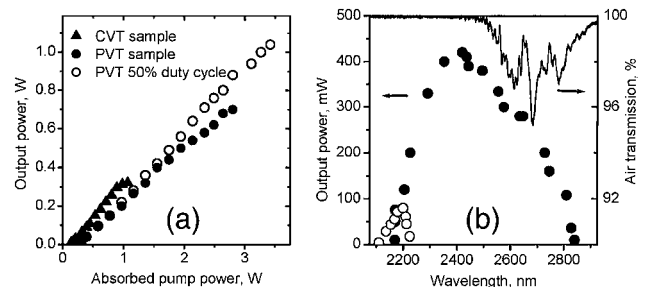


Fig. 2. (a) Output characteristics of different Cr:ZnS samples under Er-fiber laser pumping and 10% output coupling. (b) Tuning of the PVT sample under Er-fiber laser pumping. The filled and open circles refer to different mirror sets, centered at 2400 and 2100 nm, respectively. The solid curve shows air transmission, normalized to the resonator length.

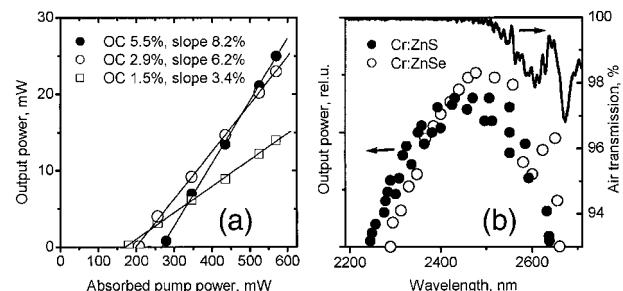


Fig. 3. (a) Output characteristics of Cr:ZnS laser (PVT sample) under diode pumping. (b) Tuning curves of the PVT Cr:ZnS (filled circles) and of the PVT Cr:ZnSe (open circles) under diode pumping. The solid curve shows air transmission, normalized to the resonator length.

to water absorption as well as the etalon effect of the air gap between the crystal surface and the input mirror. The oscillation linewidth was measured to be less than 0.4 nm (<20 GHz).

Since the spectral luminescent parameters of the Cr:ZnS sample are close to those of the Cr:ZnSe, we explain the lower efficiency and higher threshold of Cr:ZnS by the higher passive losses. Although the measured losses of 14%/cm ( $7 \pm 1.5\%$  per round trip though the 2.5-mm-thick crystal) are lower than the corresponding value of 27%/cm for the CVT-grown Cr:ZnS (5.5% per round trip through the 1-mm-thick crystal), which was studied previously,<sup>9</sup> they are still considerably higher than in Cr:ZnSe ( $\sim 4\%/cm$ ).<sup>3</sup> This means that improvement in the crystal growth and diffusion-doping techniques of Cr:ZnS should lead to improvement of the laser parameters up to at least the level of Cr:ZnSe, with the advantage of lower  $dn/dT$  (+46 versus +70  $\times 10^{-6}/^{\circ}\text{C}$ ; Ref. 1) as well as a larger bandgap. The latter decreases the probability of multiphoton absorption at high intensity.

Finally, as an interesting observation we would like to mention the sensitivity of the output radiation of the Cr:ZnS laser to low-power (a few milliwatts) excitation in the visible wavelength range. Depending on the wavelength of this additional excitation, the output power either increases or decreases. This phenomenon was first observed in diode-pumped Cr:ZnSe.<sup>8</sup> Its origin is the multivalence character of transition-metal ions in chalcogenides and the effective charge transfer involving chromium ions. The transition-metal ions, depending on the valency and position of their energy levels in the bandgap, act as either deep-level donors or acceptors needed for photorefraction. A typical example is vanadium-doped CdMnTe, in which Brost *et al.* observed the photorefractive effect<sup>16</sup> when it was excited in the visible and the near infrared. In our experiment with Cr:ZnS, we observed an increase of the laser output power when the sample was additionally excited by  $\sim 5$  mW in the wavelength range from 740 to 770 nm and a decrease of the output power when the sample was excited by 5–10 mW at  $\lambda < 520$  nm ( $\lambda = 476, 488, 496$  nm). This observation deserves a separate study. Here we note only that these two experimentally determined excitation bands [which are wavelength shifted from the analogous bands in Cr:ZnSe (see Ref. 8) in accordance with the position of the charge-transfer bands] correspond to the following charge-transfer processes (for a list of references, see Ref. 8):  $\text{Cr}^{2+} + h\nu \rightarrow \text{Cr}^{1+} + h\nu_{\text{VB}}$  and  $\text{Cr}^{1+} + h\nu \rightarrow [\text{Cr}^{2+}]^* + e_{\text{CB}}$ , where  $h\nu_{\text{VB}}$  and  $e_{\text{CB}}$  denote a hole in the valence band and an electron in the conduction band, respectively. Using this model, we can then explain the decrease of the laser output power as a reduction of the active-ion concentration in the first process and growth of the output power as a decrease of the active ion concentration as a result of the second process. The quantum yield of the latter is quite low [4% for Cr:ZnSe (Ref. 17)]. However, even a small increase of the number of active ions in the four-level Cr:ZnS laser noticeably affects its output power. This observation, as in the case of Cr:ZnSe, is potentially useful for optical switching.

In conclusion, we have demonstrated what is to our knowledge the first directly diode-pumped cw Cr:ZnS laser that is broadly tunable over  $\sim 400$  nm. Another compact but relatively more expensive Er-fiber-pumped version of the Cr:ZnS laser, yielding 0.7 W of polarized TEM<sub>00</sub> radiation that is tunable over  $\sim 700$  nm at 34% slope efficiency, demonstrates the good power-handling capability of this laser crystal.

We thank Kurt Mereiter for the x-ray analysis. This work was performed under FWF grants T64 and P14704-TPH and BMBWK grant B631. I. Sorokina's e-mail address is sorokina@tuwien.ac.at.

## References

1. L. D. DeLoach, R. H. Page, G. D. Wilke, S. A. Payne, and W. P. Krupke, *IEEE J. Quantum Electron.* **32**, 885 (1996).
2. G. J. Wagner, T. J. Carrig, R. H. Page, K. I. Schaffers, J. Ndad, X. Ma, and A. Burger, *Opt. Lett.* **24**, 19 (1999).
3. I. T. Sorokina, E. Sorokin, A. DiLieto, M. Tonelli, R. H. Page, and K. I. Schaffers, *J. Opt. Soc. Am. B* **18**, 926 (2001).
4. T. J. Carrig, G. J. Wagner, A. Sennaroglu, J. Y. Jeong, and C. R. Pollock, *Opt. Lett.* **25**, 168 (2000).
5. I. T. Sorokina, E. Sorokin, A. DiLieto, M. Tonelli, R. H. Page, and K. I. Schaffers, in *Advanced Solid-State Lasers*, S. Payne and C. Marshall, eds., Vol. 46 of OSA Trends in Optics and Photonics Series (Optical Society of America, Washington, D.C., 2001), p. 157.
6. E. Sorokin, I. T. Sorokina, and R. H. Page, in *Advanced Solid-State Lasers*, S. Payne and C. Marshall, eds., Vol. 46 of OSA Trends in Optics and Photonics Series (Optical Society of America, Washington, D.C., 2001), p. 101.
7. A. V. Podlipensky, V. G. Shcherbitsky, N. V. Kuleshov, V. I. Levchenko, V. N. Yakimovich, M. Mond, E. Heumann, G. Huber, H. Kretschmann, and S. Kück, *Appl. Phys. B* **72**, 253 (2001).
8. E. Sorokin and I. T. Sorokina, *Appl. Phys. Lett.* **80**, 3289 (2002).
9. I. T. Sorokina, E. Sorokin, V. Fedorov, S. Mirov, A. DiLieto, M. Tonelli, V. Badikov, and V. Panyutin, "Continuous-wave tunable Cr<sup>2+</sup>:ZnS laser," *Appl. Phys. B* (to be published).
10. S. Mirov, V. V. Fedorov, K. Graham, I. S. Moskalev, V. Badikov, and V. Panyutin, *Opt. Lett.* **27**, 909 (2002).
11. A. A. Berezhnoi, Yu. V. Popov, T. N. Sherstneva, and V. M. Solntsev, *Opt. Spektrosk.* **43**, 286 (1977).
12. N. D. Nedashkovskaya, *Opt. Spektrosk.* **55**, 584 (1983).
13. R. M. Akopyan, V. N. Bagdavidze, O. V. Gogolin, and E. G. Tsitsishvili, *Sov. Phys. Semicond.* **20**, 903 (1986).
14. G. J. Wagner and T. J. Carrig, in *Advanced Solid-State Lasers*, S. Payne and C. Marshall, eds., Vol. 46 of OSA Trends in Optics and Photonics Series (Optical Society of America, Washington, D.C., 2001), p. 506.
15. J. A. Caird, S. A. Payne, P. R. Staver, A. J. Ramponi, L. L. Chase, and W. F. Krupke, *IEEE J. Quantum Electron.* **QE-24**, 1077 (1988).
16. G. A. Brost, K. M. Magde, and S. Trivedi, *Opt. Mater.* **4**, 224 (1996).
17. A. V. Vasil'ev, S. A. Kazanskii, and A. I. Ryskin, *Opt. Spektrosk.* **84**, 410 (1998).